

1 **Long-term changes of nitrogen leaching and ~~their~~ the contributions of**
2 **terrestrial nutrient sources to lake eutrophication dynamics on the Yangtze**
3 **Plain of China**

4 **Qi Guan^{a, b, c}, Jing Tang^{d, e, *}, Lian Feng^b, Stefan Olin^d, Guy Schurgers^c**

5 ^a Taihu Laboratory for Lake Ecosystem Research, State Key Laboratory of Lake Science and
6 Environment, Nanjing Institute of Geography and Limnology, Chinese Academy of Sciences, Nanjing
7 210008, China.

8 ^b School of Environmental Science and Engineering, Southern University of Science and Technology,
9 Shenzhen 518055, Guangdong, China.

10 ^c Department of Geosciences and Natural Resource Management, University of Copenhagen,
11 Copenhagen, Denmark.

12 ^d Department of Physical Geography and Ecosystem Science, Lund University, Lund, Sweden.

13 ^e Department of Biology, University of Copenhagen, Copenhagen, Denmark.

14 * ~~corresponding~~ Corresponding author: jing.tang@nateko.lu.se

15 **Abstract**

16 Over the past ~~half-century~~ half-century, drastically increased chemical ~~fertilizers~~ fertilizer have entered
17 agricultural ecosystems to promote ~~the~~ crop production on the Yangtze Plain, potentially enhancing
18 agricultural nutrient sources for eutrophication in freshwater ecosystems. However, long-term trends of
19 nitrogen dynamics in terrestrial ecosystems and their impacts on eutrophication changes in this region
20 remain poorly studied. Using a process-based ecosystem model, we investigated the temporal and
21 spatial patterns of nitrogen use efficiency (NUE) and nitrogen leaching on the Yangtze Plain from 1979
22 to 2018. The agricultural NUE for the Yangtze Plain significantly decreased from 50 % in 1979 to 25%
23 in 2018, with the largest decline of NUE in soybean, rice and rapeseed. Simultaneously, the leached
24 nitrogen from cropland and natural land increased with annual rates of 4.5 kg N ha⁻¹ yr⁻² and 0.22 kg N
25 ha⁻¹ yr⁻², respectively, leading to an overall increase of nitrogen inputs to the fifty large lakes. We further
26 examined the correlations between terrestrial nutrient sources (i.e., the leached nitrogen, total

27 phosphorus sources, and industrial wastewater discharge) and the satellite-observed probability of
28 eutrophication occurrence (PEO) at an annual scale, and showed that PEO was positively correlated
29 with the changes in terrestrial nutrient sources for most lakes. Agricultural nitrogen and phosphorus
30 sources were found to explain the PEO trends in lakes in the western and central part of [the](#) Yangtze
31 Plain, and industrial wastewater discharge was associated with the PEO trends in eastern lakes. Our
32 results revealed the importance of terrestrial nutrient sources for long-term changes in eutrophic status
33 over the fifty lakes of the Yangtze Plain. This calls for [region-specific](#) sustainable [nutrient management](#)
34 [\(i.e., nitrogen and phosphorus applications in agriculture and industry\)](#) to improve [the](#) water quality of
35 lake ecosystems.

36 **1 Introduction**

37 For the past [half-century](#)~~half-century~~, China's demand for grain production has increased from 250 Mt
38 in 1960 to 648 Mt in 2010 along with the growing population, industrial development, and human-diet
39 changes (Zhao et al., 2008; Wang and Davis, 1998). Substantial chemical fertilizers (i.e., 35 mega-tons,
40 Mt, nitrogen fertilizers in 2014 (Yu et al., 2019) simultaneously entered agricultural ecosystems for the
41 promotion of crop production. Although national grain production consequently increased from 132 Mt
42 in 1950 to 607 Mt in 2014 (Yu et al., 2019), such a level of fertilization has enhanced nitrogen discharge
43 to terrestrial and freshwater ecosystems, leading to a series of ecological and environmental concerns,
44 such as soil nitrogen pollution, water quality deterioration, and phytoplankton blooms (Zhang et al.,
45 2019; Wang et al., 2021b; Qu and Fan, 2010). It was reported that approximately 14.5 Mt N yr⁻¹ was
46 discharged to surface water ecosystems over ~~the~~ [entire of](#) China for the period of 2010-2014, which
47 largely exceeded the national safe level of nitrogen discharge (i.e., 5.2 Mt N yr⁻¹) for the aquatic
48 environment (Yu et al., 2019). Such human-related nutrient enrichment poses a big challenge ~~to~~[for](#)
49 China's sustainable development goals (Wang et al., 2022).

50 The Yangtze Plain, with a human population of 340 million and [an](#) agricultural area of 100 million
51 hectares (Chen et al., 2020b; Hou et al., 2020), is experiencing unprecedented ecological and
52 environmental issues (Guan et al., 2020; Feng et al., 2019). From 1990 to 2015, total crop production
53 increased by 15 % at the expense of an increase of 89 % in nitrogen fertilizers over the Yangtze Plain

54 (Xu et al., 2019). Consequently, more frequent nitrogen pollution was observed in soil and water. For
55 example, heavy fertilizer usage and intensive livestock contributed to soil nitrogen pollution ~~in~~ the
56 Yangtze River Delta for the past four decades, leading to soil deterioration and nitrogen discharge (Zhao
57 et al., 2022). Nitrogen discharge related to human activities (i.e., fertilizer and manure applications, and
58 human food waste) largely increased the nutrient loading and accelerated the degradation of water
59 quality in the Yangtze River since the 1990s (Chen et al., 2020c). Under the recent sustainable
60 development plans proposed by national and local governments, managing nitrogen sources from urban
61 and crop systems is envisaged to mitigate severe soil and water ~~pollution~~ ~~pollutions~~ (Chen et al., 2020c;
62 Zhao et al., 2022; Shi et al., 2020). However, for the Yangtze Plain with a variety of crops and crop
63 ~~management~~ ~~managements~~, the lack of insights into long-term changes ~~in~~ ~~of~~ nitrogen dynamics, such as
64 fertilizer application, plant nitrogen uptake, and nitrogen leaching, has limited our solution of proposing
65 effective policies related to nutrient management.

66 In recent several decades, national field surveys and satellite observations have been widely used to
67 investigate nutrient loadings (Tong et al., 2017; Li et al., 2022), chlorophyll-a concentrations (Guan et
68 al., 2020), trophic state index (TSI) (Hu et al., 2022; Chen et al., 2020a) and algal bloom occurrence
69 (Huang et al., 2020) to assess eutrophication issues in local or regional lakes of the Yangtze Plain, all
70 of which revealed the lakes on the Yangtze Plain experienced eutrophication and algal blooms for the
71 past two decades. According to the national surveys and satellite observations, the lakes on the Yangtze
72 Plain experienced eutrophication and algal blooms for the past two decades (Guan et al., 2020; Li et al.,
73 2014; Hu et al., 2022). Cyanobacteria blooms were reported to frequently occur in Taihu and Chaohu
74 lakes, with the peak expanded extent reported for 2006 (Qin et al., 2019). Since then, the magnitudes
75 of algal blooms significantly decreased from 2006 to 2013, and slightly increased again from 2013 to
76 2018 (Huang et al., 2020). Satellite observations revealed widespread and serious eutrophication issues
77 in large lakes of the Yangtze Plain for the periods of 2003-2011 and 2017-2018, although significantly
78 decreasing trends were found in 20 out of 50 lakes throughout the periods (Guan et al., 2020). Moreover,
79 35-year Landsat-derived trophic state index (TSI) also indicated that hyper-eutrophic and eutrophic
80 lakes mainly characterized the Yangtze Plain, with slight increase in TSI from 1986 to 2012 and then

81 decrease since 2012 (Hu et al., 2022). National field surveys demonstrated that although total
82 phosphorus concentrations overall decreased from 2006 to 2014, it still remained under high levels
83 (i.e., > 50 $\mu\text{g L}^{-1}$) in eastern China lakes (Tong et al., 2017). Various laws and guidelines were
84 implemented on regional and national scales to control eutrophication problems, such as the Guidelines
85 on Strengthening Water Environmental Protection for Critical Lakes in 2008 and the Water Pollution
86 Control Action Plan in 2015 (Huang et al., 2019). Nevertheless, the eutrophication issues are still
87 challenging to control and improve under the scarcity of effective strategies for the whole Yangtze Plain
88 due to unknown causes of eutrophication issues.

89 To understand the primary causes of eutrophication in the lakes of the Yangtze Plain, previous studies
90 have attempted to determine the contributions of riverine nutrient exports and lacustrine nutrient loading
91 to algal blooms in individual lakes, such as Taihu and Chaohu lakes (Tong et al., 2017; Tong et al.,
92 2021; Xu et al., 2015). Based on field-measured phytoplankton biomass and nutrient concentrations,
93 algal blooms in Taihu Lake were primarily attributed to excessive nutrient loads from 1993 to 2015
94 (Zhang et al., 2018). Overloaded nutrients, in combination with climatic warming, were found to
95 regulate the seasonal variations of cyanobacteria blooms in Chaohu Lake based on the monthly nutrient
96 monitoring at discrete points (Tong et al., 2021). However, these studies only tracked the primary
97 drivers of algal blooms for individual hyper-eutrophic lakes (i.e., Taihu and Chaohu lakes), which is
98 insufficient to understand regional variations in terms of the causes of eutrophication and support the
99 design of effective management strategies to mitigate eutrophication issues across different eutrophic
100 states of lakes. Furthermore, lacustrine nutrient loading is always associated with terrestrial nutrient
101 sources, such as synthetic fertilizers, livestock manure, and industrial sewage (Wang et al., 2019b; Yu
102 et al., 2018). For example, Wang et al. (2019b) identified that diffuse sources contributed 90% to
103 riverine exports of total dissolved nitrogen, and point sources discharged 52% of riverine phosphorus
104 exports to Taihu Lake, where diffuse sources are synthetic fertilizers and atmospheric deposition, and
105 point sources are sewage and manure discharge. It was also reported that chemical fertilizer and
106 wastewater discharge provided primary nitrogen sources for the Chaohu Lake (Yu et al., 2018).
107 Unfortunately, all these studies did not examine the impacts of vegetation uptake and soil retention on

~~terrestrial nutrient sources, making it insufficient to comprehensively understand the linkage between terrestrial nutrient sources and eutrophication in regional lake ecosystems. Additionally, the studies above investigate cyanobacteria dynamics in relation to regional fertilizer use, but do not quantify changes in nitrogen uptake by vegetation.~~

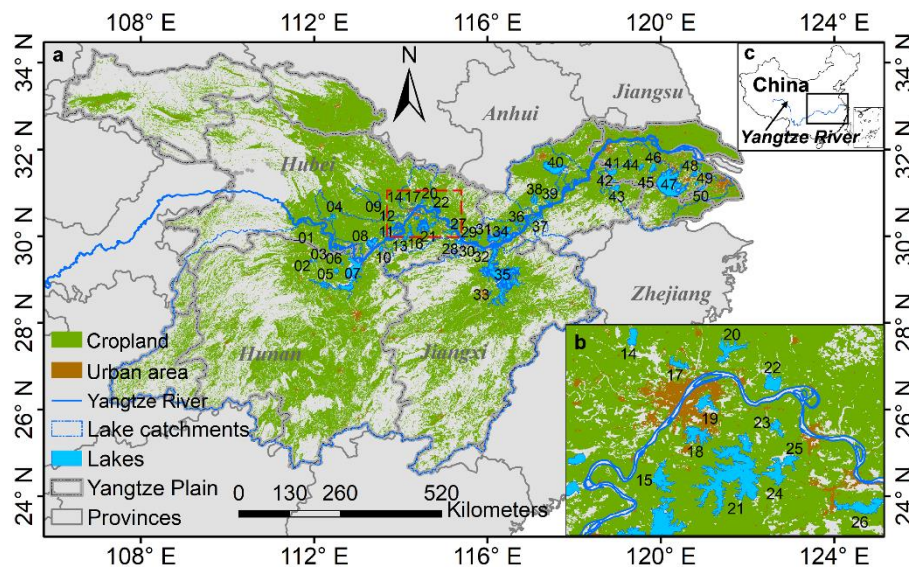
In this study, we employed a process-based dynamic vegetation model, LPJ-GUESS (Smith et al., 2014), to investigate terrestrial nitrogen dynamics for the past four decades, examining the primary drivers of eutrophication trends in fifty large lakes of the Yangtze Plain (covering 63% of the whole plain). We simulated the vegetation dynamics, nitrogen cycles for agricultural and natural ecosystems from 1979 to 2018, and then assessed the temporal trends of nitrogen use efficiency and nitrogen leaching. The terrestrial nutrient sources were used to examine their linkage with the satellite-derived eutrophication changes for fifty large lakes.

2 Materials and Methods

2.1 Study area

The Yangtze Plain (Fig. 1) is in the middle and lower basin of the Yangtze River. It covers a total area of 7.8×10^6 km² from Hunan Province to Shanghai City, and accommodates approximately 5000 freshwater lakes, ponds and reservoirs (Hou et al., 2017). Its sub-tropical monsoon climate provides annual mean temperature (~15°C) and precipitation (~1000 mm) conditions favorable for crop cultivation, in particular cereals and oil seeds, making the Yangtze Plain one of the top three food production regions in China. Generally, rice-sown area contributed dominantly to agriculture areas associated with climate conditions and human dietary (Piao et al., 2010; Tilman et al., 2011). To enhance crop production, double-cropping strategy has been widely implemented on the Yangtze Plain, such as the rotation of early- and late-season rice (Chen et al., 2017), and the rotation of summer maize and winter wheat (Xiao et al., 2021). Several common management practices were adopted by millions of smallholders (Cui et al., 2018). For example, straw return, organic manure applications, and suitable planting density were also recommended in recent years (Cui et al., 2018). Significantly increased fertilizer applications to cropland were expected to stimulate crop yield over the past half century (Yu

134 et al., 2019; Zhang et al., 2015). Such management practice can certainly enhance agriculture
 135 productivity, but also cause negative consequences to soil and aquatic environment (Liu et al., 2016a;
 136 Shi et al., 2020). However, since the policy of Reform and Opening-up of China in the 1980s (Zhang
 137 et al., 2010), agricultural ecosystems have been confronted with great pressure from urban expansion
 138 on the Yangtze Plain. Rapid urban expansion encroached on arable land, mainly on the eastern parts of
 139 the Yangtze Plain (Zhang et al., 2021).



140

141 **Figure 1.** Locations of the Yangtze Plain and the fifty large lakes studied here. (b) Detailed overview
 142 of Wuhan region (red box in (a)) and the surrounding lakes.

143 2.2 Dynamic vegetation model

144 We used a dynamic ecosystem model, LPJ-GUESS (Smith et al., 2014; Olin et al., 2015b), to simulate
 145 vegetation dynamics (i.e., the establishment, growth, competition, and mortality of plants), soil
 146 biogeochemistry, and carbon and nitrogen cycles for different ecosystems on the Yangtze Plain. The
 147 model has been widely used to assess ecosystem carbon and nitrogen fluxes at regional and global scales
 148 (Smith et al., 2014). Plant functional types (PFTs) and crop functional types (CFTs) are designed to
 149 describe the different types of plants and crops with a set of pre-defined bioclimatic and physiological
 150 parameters, such as photosynthetic pathways, phenology, growth forms and life history strategies for

151 PFTs, as well as irrigation, fertilization, and rotation schemes for CFTs (Smith et al., 2014; Sitch et al.,
152 2003; Olin et al., 2015a; Lindeskog et al., 2013).

153 Carbon and nitrogen fluxes between ecosystems and the atmosphere are calculated on a daily basis. For
154 natural PFTs, net primary production (NPP) is accumulated and allocated to different plant
155 compartments (i.e., leaves, roots, sapwood and heartwood for trees) at the end of each simulation year.
156 Soils are represented by 11 carbon and nitrogen pools with different decomposition rates (Parton et al.,
157 1993; Parton et al., 2010), dependent on soil temperature and texture, water content, and base decay
158 rates (Smith et al., 2014). Atmospheric deposition and plant biological fixation provide nitrogen sources
159 for plant growth and development, while the decomposition of soil organic matter can release -mineral
160 N into the [soil](#) and nitrogen-related gases into the atmosphere. Moreover, soluble nitrogen [in soil](#) can
161 also leach with the surface runoff in the forms of dissolved organic and inorganic nitrogen (i.e., DON
162 and DIN). In the model, leaching of DON is a function of the decay rates of soil microbial carbon pool
163 and soil percolation, while DIN leaching depends on the available mineral nitrogen in soils and soil
164 percolation, as well as soil water content.

165 Crop growth starts from a seedling with initial carbon and nitrogen masses at a prescribed sowing date.
166 Chemical fertilizer and livestock manure supply external nitrogen for crop growth. [According to local
167 farmers' practice \(Shi et al., 2020\), chemical fertilizer and manure applications are often applied at three
168 different stages: sowing, tillering, and heading stages. Such fertilization schemes are also represented
169 in the LPJ-GUESS \(Olin et al., 2015a\), where nitrogen fertilizer is applied when the crop development
170 stage reaches 0, 0.5, and 0.9 in response to three above stages, and the relative fertilization rate for each
171 stage are empirical parameters based on field surveys.](#) Crop N uptake is simulated as the lesser between
172 crop N demand and accessible mineral N in soils, where the former depends on crop development stages
173 and C:N ratios of leaves and roots, and the latter is affected by soil temperature and fine root biomass
174 (Olin et al., 2015a). Differing from natural PFTs, NPP is allocated to leaves and stems, root, and storage
175 organs for each CFT on a daily basis, according to the daily allocation strategies related to crop
176 development stages (Olin et al., 2015a).

177 2.3 LPJ-GUESS input, calibration, and evaluation dataset

178 2.3.1 Input data

179 We ran LPJ-GUESS separating four land use types (natural land, cropland, pasture and urban) with a
180 500-year spin-up to simulate the vegetation dynamics and the associated nitrogen fluxes for the Yangtze
181 Plain from 1979 to 2018.

182 The gridded input data for LPJ-GUESS include climate, fractions of four land use types, total chemical
183 fertilizer and manure application rates, cover fractions of each CFT within the cropland area, and soil
184 properties. We used daily temperature, precipitation, and shortwave radiation provided by the China
185 Meteorological Forcing Dataset (CMFD), with a spatial resolution of 0.1° and a temporal coverage of
186 1979-2018 (He et al., 2020). The 300-m Climate Change Initiative Land Cover (CCI-LC version 2.0)
187 dataset was regrouped into four different land use types (i.e., urban, cropland, pasture, and natural land)
188 to obtain the cover fractions within each 0.1° grid cell for the period of 1992 to 2018 (Defourny et al.,
189 2012) (see the details about regrouping process in Supplementary S1). Soil properties, i.e., fractions of
190 sand, clay and silt, organic carbon content, C:N, pH, and bulk density were extracted from the World
191 Inventory of Soil Property Estimates (WISE30sec) dataset (Batjes, 2016). Based on the original data
192 with a spatial resolution of 30 sec, we determined the dominant FAO soil type based on their relative
193 area in each grid cell, and used its properties as input data for the grid cell. Gridded chemical fertilizer
194 and manure application data were extracted from global fertilizer usage (Lu and Tian, 2017) and manure
195 data (Zhang et al., 2017), which have spatial resolutions of 0.5° and $0.5'$, respectively. We resampled
196 the fertilizer and manure application data into the spatial resolution of 0.1° to represent the chemical
197 fertilizer and manure application for each grid cell from 1979 to 2014. The gridded monthly N
198 deposition data were also extracted from an external database as an input file (Lamarque et al., 2013).
199 It has a spatial resolution of 0.5° , and we used the value in the nearest grid cell to represent N deposition
200 in the simulations.

201 The gridded fractions of CFTs were calculated based on observational data provided by the China
202 Meteorological Data Service Center (<https://data.cma.cn/site/subjectDetail/id/101.html>). The dataset

203 contains the information about the types, sowing and harvest dates for [a total of](#) eleven crops at 92
204 observational sites across the whole Yangtze Plain (listed in Table S1). An adaptive inverse distance
205 weighting method was then used to interpolate the maps of the relative fractions of all crops, and their
206 sowing and harvest dates for the period of 1992-2015 (see the details in Supplementary S2). Due to the
207 limited availability for the period of 1979-1991 and 2016-2018, we used the same crop information (i.e.,
208 the fractions of crop types, sowing and harvest dates) from the nearest years.

209 **2.3.2 Model calibration and evaluation data**

210 The model was calibrated based on the observed crop yield collected by the China Meteorological Data
211 Service Center (<https://data.cma.cn/site/showSubject/id/102.html>). The dataset provides crop yield data
212 for eight main crops collected at different numbers of sites (i.e., winter wheat (number of sites: 37),
213 spring maize (6), summer maize (10), single-season rice (28), early-season rice (30), late-season rice
214 (30), rapeseed (38), and soybean (15)), for the period of 2000-2013. For the Yangtze Plain, hybrid and
215 super-hybrid rice are widely cultivated to obtain high grain yield within short growing seasons due to
216 the enhanced photosynthetic rates associated with leaf-level chlorophyll and rubisco contents (Huang
217 et al., 2016). However, the default parameters for rice CFTs in LPJ-GUESS cannot capture the [high-](#)
218 [yield](#) features of hybrid and super-hybrid rice. Therefore, we calibrated the relationship between the
219 leaf-based nitrogen content and the maximum catalytic capacity of rubisco (see the details in
220 Supplementary S3). We randomly selected five sites with rice yield data from 2000 to 2013 as the
221 calibration data, and the other rice yield data were used as the evaluation data. For parameters of other
222 CFTs (listed in Table S1), the default values performed [satisfactorily](#) in the comparison with all
223 observed yield data (Fig. 2). It is noted that regional mean yield for each crop was derived from the
224 evaluation data to compare the simulated values on the Yangtze Plain.

225 Simulated GPP and LAI were further compared with Global Solar-induced Chlorophyll Fluorescence
226 Gross Primary Productivity (GOSIF GPP) and third generation of Global Inventory Modeling and
227 Mapping Studies Leaf Area Index (GIMMS LAI3g) products to evaluate the performance of modelled
228 vegetation variables. The global GOSIF GPP products have a spatial resolution of 0.05° and cover the
229 period of 1992-2018 (Li and Xiao, 2019). Biweekly GIMMS LAI3g products with a spatial resolution

230 of 0.25° were obtained and then converted to annual mean LAI3g maps from 1982 to 2011 (Zhu et al.,
231 2013).

232 The modelled responses of nitrogen leaching to different fertilizer applications were evaluated based
233 on an observational dataset published by Gao et al. (2016), where they collected nitrogen leaching for
234 plots with 3 or 4 different levels of nitrogen fertilizer inputs for maize, rice, and wheat. In our study, we
235 selected the observed responses without influences of phosphorus and potash fertilizers on the Yangtze
236 Plain as the evaluation data (two samples for each crop). For these sites, individual simulations were
237 performed by assigning the full coverage of each corresponding crop growth and prescribing the levels
238 of nitrogen fertilizer applications as in the experimental site. It should be noted that we used the same
239 nitrogen fertilizer applications in the period prior to the field experiment.

240 **2.4 Assessment of long-term changes in nitrogen dynamics**

241 We assessed long-term changes in nitrogen use efficiency (NUE) and nitrogen leaching over the past
242 four decades. ~~For the LPJ-GUESS simulated NUE and leached nitrogen, a~~ linear regression was
243 conducted ~~for on~~ the annual mean ~~NUE and leached nitrogen values~~ for the whole Yangtze Plain to
244 determine the associated change rates (i.e., the regression slopes), and the significance was tested by a
245 *t*-test. The mean leached nitrogen over the drainage area of all examined lakes was calculated to explore
246 long-term changes in terrestrial nitrogen sources for lake ecosystems, and the associated temporal trends
247 were assessed by the linear regression and *t*-test.

248 **2.5 Examination of the primary driving forces of eutrophication dynamics**

249 **2.5.1 Satellite-derived eutrophication changes**

250 We used satellite-derived PEO data published in Guan et al. (2020) to represent the eutrophication
251 changes for fifty large lakes on the Yangtze Plain. The PEO was defined as the frequency of high
252 chlorophyll-a concentrations (i.e., > 10 mg m⁻³) or algal bloom occurrences in satellite imagery for each
253 year. ~~All full-resolution (300 m) MERIS and OLCI images were used to derive chlorophyll-a~~
254 ~~concentrations by using a SVR-based piecewise retrieval algorithm, and also detect algal bloom through~~
255 ~~two indices. High temporal resolutions for MERIS (i.e., 3 days) and OLCI (i.e., 1-2 days) ensure to~~

256 provide sufficient observations on rapidly dynamic lake ecosystems. The averaged PEO values for
257 pixels within each lake were then obtained to delineate the eutrophication status and changes in fifty
258 large lakes of the Yangtze Plain during the MERIS (i.e., 2003-2011) and OLCI (i.e., 2017-2018)
259 observational periods. However, due to the unavailability of the crop- and nitrogen-related data for the
260 period of 2017-2018, we only used the PEO data derived from MERIS observations (i.e., 2003-2011)
261 here to examine their primary driving forces.

262 **2.5.2 Examination of the correlations between nutrient and PEO anomalies**

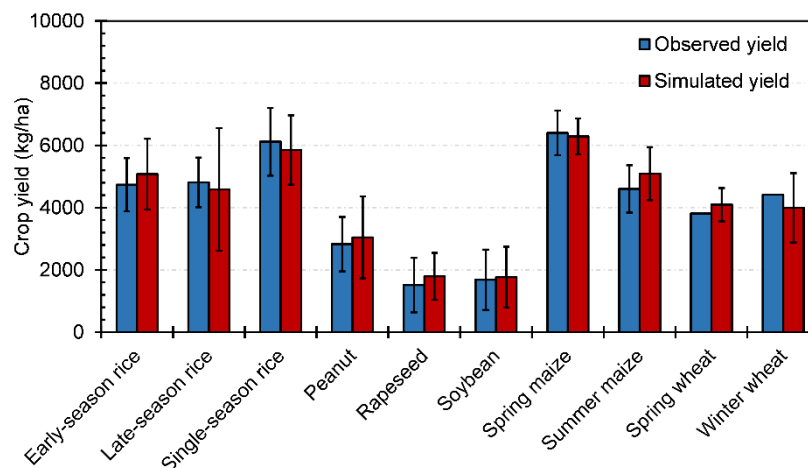
263 To examine the impacts of terrestrial nutrient sources on eutrophication changes in fifty large lakes of
264 the Yangtze Plain, we used the simulated nitrogen leaching (LN) and anthropogenic phosphorus sources
265 (i.e., total phosphorus from chemical fertilizer and manure, TP) representing the agricultural nutrient
266 sources, and industrial wastewater discharge (IW) representing industrial nutrient sources. The gridded
267 phosphorus fertilizer data were extracted from a global dataset developed by Lu and Tian (2017), while
268 the phosphorus content in manure was calculated based on the nitrogen contents of manure products
269 and the associated N:P ratios of different animals' excrement (Table S3). Annual industrial wastewater
270 discharge data were obtained from the China City Statistical Yearbook ([https://data.cnki.net/trade/Year-](https://data.cnki.net/trade/Year-book/Single/N2018050234?zcode=Z011)
271 [book/Single/N2018050234?zcode=Z011](https://data.cnki.net/trade/Year-book/Single/N2018050234?zcode=Z011)). Note that both agricultural phosphorus sources and
272 industrial wastewater discharge are inventory data.

273 The 9-year mean (2003-2011) of three nutrient-related variables (i.e., LN, TP and IW) was/were used in
274 a principal component analysis (PCA) followed by a K-means clustering (Hartigan and Wong, 1979)
275 to classify examined fifty lakes based on similarities of terrestrial nutrient sources. In this process, all
276 variables were normalized (across all years and lakes) based on the z-score method to remove the
277 influence of different magnitudes in nutrient-related variables. We derived the first two principal
278 components (PCs) from all normalized variables through a PCA, and the lakes were classified into three
279 classes based on the first two PCs through the clustering methods. Finally, the annual anomalies of these
280 nutrient-related variables and PEOs relative to their 9-year means were used to determine the primary
281 drivers of temporal trends in eutrophication for each lake class.

282 3 Results

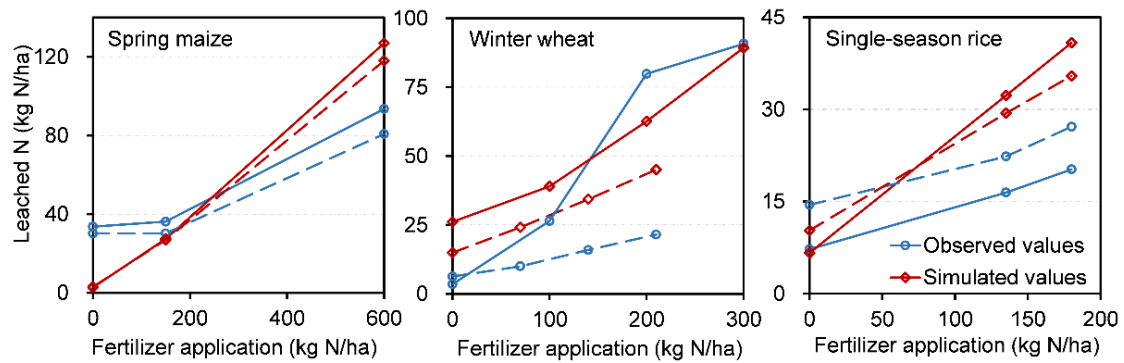
283 3.1 Evaluation of LPJ-GUESS simulation

284 For the evaluation of LPJ-GUESS simulation for the past four decades, the simulated LAI, GPP and
285 crop yield were compared with observation-based estimates. Mean crop yields agreed well with the
286 observed values, with mean relative errors of < 10% (Fig. 2). The comparison of simulated and observed
287 LAI, and GPP were also satisfactory with overall high accuracy (i.e., a mean relative error of ~20% and
288 the root squared relative errors of < 30%) and spatial distributions consistent with observed patterns
289 (Fig. S1 and S2). Considering the difference in spatial scales between the grid cells and the gridded
290 evaluation data (i.e., the observed LAI and GPP maps), the overall performance of vegetation simulation
291 over the different land use types ~~was~~ considered acceptable. In addition, the simulated responses
292 of nitrogen leaching to different fertilizer applications at the experimental sites showed overall similar
293 trends as the observation ones for all three crops (i.e., maize, rice, and wheat), despite varying
294 magnitudes of differences between the simulated and observed leached nitrogen at certain fertilizer
295 level (Fig. 3).



296

297 **Figure 2.** Comparison between the simulated and observed crop mean yields of different crops on the
298 Yangtze Plain; the mean values were averaged over the period 2000-2015 and across totally 179 sites.
299 Error bars show one standard deviation of crop yield.



300

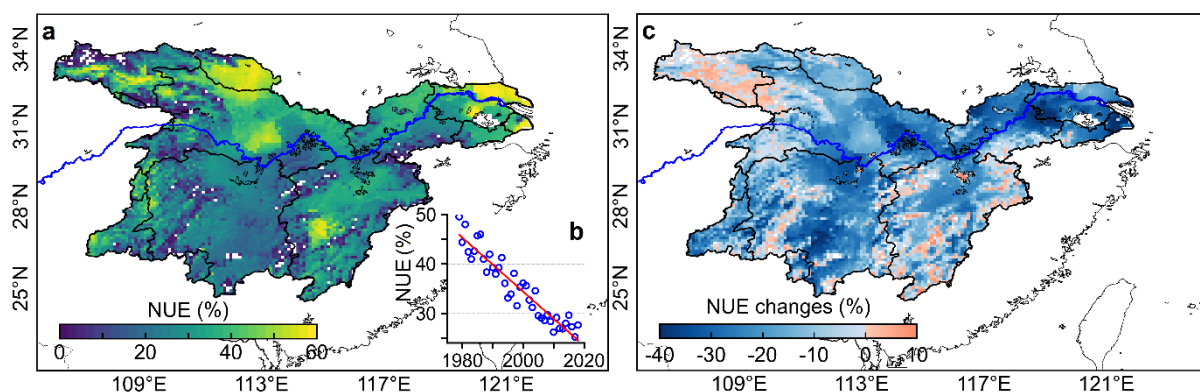
301 **Figure 3.** The simulated and observed responses of the leached nitrogen to different levels of fertilizer
 302 application rates for three main crop types (i.e., maize, rice, and wheat) over the Yangtze Plain. Note
 303 that the solid and dotted lines represented two different pairs of simulated and observed response of
 304 leached nitrogen, respectively.

305 3.2 Long-term changes of nitrogen use efficiency over the Yangtze Plain

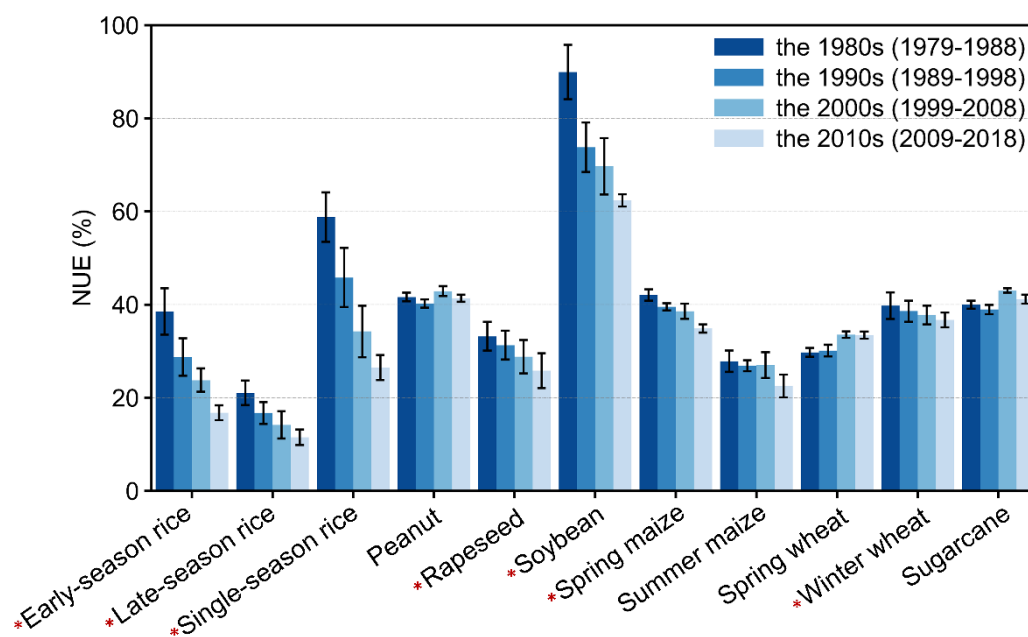
306 The climatological-average NUE for 1979 to 2018 was calculated to examine the spatial patterns of
 307 plant nitrogen uptake on the Yangtze Plain, from 1979 to 2018. Considerable variations were detected
 308 across the entire Yangtze Plain, with NUE values ranging from 5% to 60% (Fig. 4a). Two hotspots of
 309 high NUE were in the Hubei and Jiangsu Province (see locations in Fig.1), dominated by cultivations
 310 of single-season rice and winter wheat under the moderate levels (i.e., $\sim 200 \text{ kg N ha}^{-1} \text{ yr}^{-1}$) of fertilizer
 311 applications (Fig. S3). The NUE values also differed among different crop types for the past four
 312 decades. The largest NUE values were found for soybean ($74.0 \% \pm 11.0 \%$, Fig 5), while the lowest
 313 values were found for late-season rice ($15.9\% \pm 4.3\%$).

314 Due to the unprecedented increase of chemical fertilizer application since the 1980s, the crop NUE on
 315 the Yangtze Plain has significantly decreased from ca. 50% in 1979 to 25% in 2018 ($p < 0.05$, in Fig.
 316 4b), with an overall annual change rate of $-0.55 \% \text{ yr}^{-1}$. Overall, regions with relatively high levels of
 317 NUE depicted a moderate or even slight increase for the past four decades, while the regions dominated
 318 low-level NUE (i.e., Hubei and Hunan provinces in Fig. 1) experienced strongly declining trends (Fig.
 319 4a&4c), as a result of the enhanced fertilizer applications. Considerable differences in magnitudes and
 320 trends of NUE were also examined among the crop types. Significant decreases (t-test, $p < 0.05$) in the

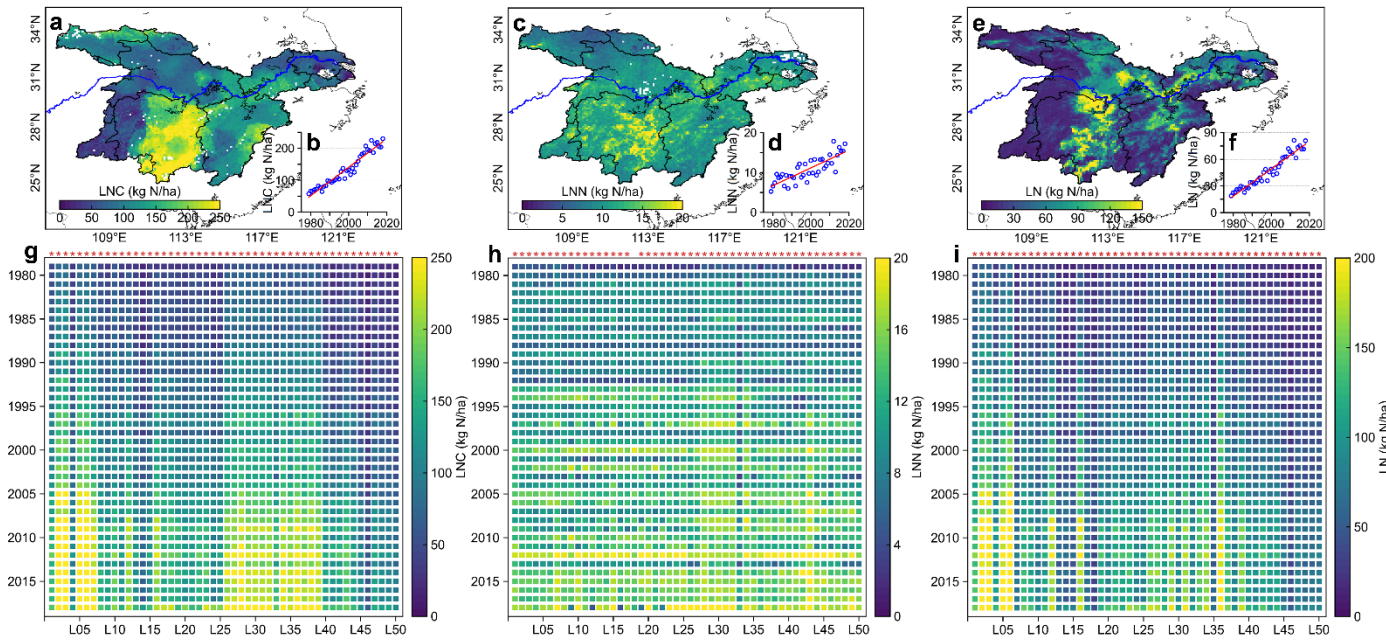
321 decadal NUEs were found for seven crop types (annotated with “*” in Fig. 5), with the largest decrease
 322 for the double cropping of early- and late-season rice (Fig. 4c and S3). In contrast, three crop types
 323 experienced increasing trends of NUE, including peanut, spring wheat, and sugarcane (Fig. 5).



324
 325 **Figure 4.** Nitrogen use efficiency (NUE) on the Yangtze Plain from 1979 to 2018. (a) Spatial
 326 distributions of climatological NUE (1979-2018), and the inset (b) shows the long-term trends of [the](#)
 327 area mean NUE; (c) Changes in NUE between the first (1979-1988) and the last (2009-2018) decades.



328
 329 **Figure 5.** Decadal values of NUE for each crop functional type, averaged over the Yangtze Plain for
 330 the past four decades. Significantly decreasing trends ($p < 0.05$) are annotated with * using a t-test.



331

332 **Figure 6.** Tempo-spatial patterns of leached nitrogen from cropland (LNC), natural land (LNN), and
 333 total leached nitrogen (LN) for the period of 1979-2018. Spatial distributions of climatological (a) LNC,
 334 (c) LNN, and (e) LN. The insets (b), (d) and (f) represent the long-term changes of mean LNC, LNN
 335 and LN, where the red lines are the linear fitting lines between years and nitrogen leaching. Inter-annual
 336 changes of (g) LNC, (h) LNN, and (i) LN for all examined lakes (L01-L50) from 1979 to 2018.
 337 Statistically significantly positive trends ($p < 0.05$) are annotated with ‘*’ on top of the panel, and see
 338 Fig. 1 for ID numbers of lakes.

339 3.3 Temporal and spatial patterns of nitrogen leaching for the past four decades

340 Along with the overall decreases in NUE, the leached nitrogen from both agricultural (LNC, averaged
 341 across cropland area) and natural systems (LNN, averaged across the natural area) experienced a
 342 statistically significant increase (t-test, $p < 0.05$) over the past four decades, with the different rates (4.5
 343 $\text{kg N ha}^{-1}\text{yr}^{-2}$ and $0.22 \text{ kg N ha}^{-1} \text{ yr}^{-2}$ derived through the linear regression, respectively in Fig. 6b, 6d).
 344 The increased LNC was primarily associated with increased fertilizer applications (increased 2.5 times
 345 from 1979 to 2018), while the increased LNN was mainly linked to enhanced atmospheric deposition
 346 (explained $75.8\% \pm 6.8\%$ of the increases in nitrogen sources) for natural ecosystems on the Yangtze
 347 Plain. The LNC were an order of magnitude larger than the LNN. The high levels of LNC were found
 348 mainly in the Hunan Province (see Fig. 1 and Fig. 6a), with an average LNC value of $149 \text{ kg N ha}^{-1} \text{ yr}^{-1}$

349 ¹. In contrast, considerable spatial variations in LNN were revealed between the north and south parts
350 of the Yangtze Plain (Fig. 6c).

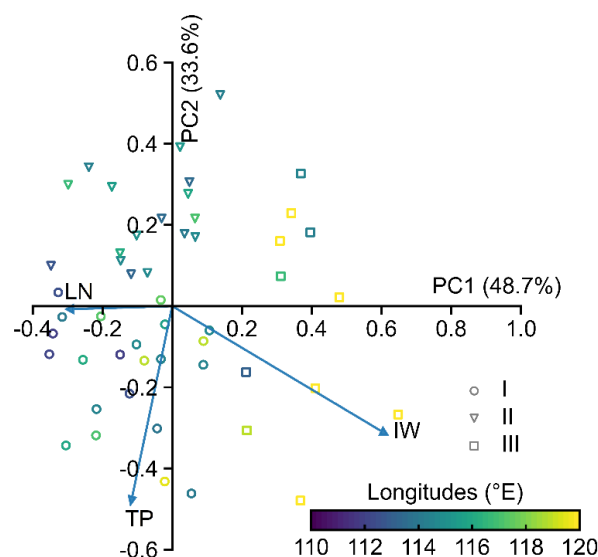
351 To understand nitrogen sources for each corresponding lake [ecosystem](#) on the Yangtze Plain, we
352 calculated the mean leached nitrogen (LN, averaged across [the ground area](#)) over the [drainage area entire](#)
353 [catchment](#) of each studied lake [provided by the HydroLAKES dataset](#) (Messenger et al., 2016). The LN
354 values ranged from 29 kg N ha⁻¹ yr⁻¹ in Gehu Lake (L46 in Fig. 6i) to 153 kg N ha⁻¹ yr⁻¹ in Donghu Lake
355 (L05 in Fig. 6i), indicating the considerable difference between the western lakes in the Hunan Province
356 and the eastern lakes in the Jiangsu Province. All examined lakes experienced statistically significantly
357 increasing trends in the LN (t-test, $p < 0.05$) over the past four decades (Fig. 6i), where the agricultural
358 activities contributed 94 % \pm 5 % to the LN changes.

359 **3.4 Driving forces of terrestrial nutrient sources to eutrophication changes**

360 The leached nitrogen ([LN](#)), total phosphorus sources ([TP](#)), and industrial wastewater discharge ([IW](#))
361 were used to represent terrestrial nutrient sources and were further investigated in terms of their [linkages](#)
362 to the observed PEOs. In the PCA analysis, the first two principal components (PCs) explained 48.7%
363 and 33.6% of variations in terrestrial nutrient sources (Fig. 7), where the first PC primarily depicts
364 positive dependence on IW but negative links with LN, and the second PC reveals negative dependences
365 on TP and IW. All fifty lakes were clustered into three classes based on the first two PCs (Fig. 7). Lakes
366 in class I (n = 22) had positive loading in the direction of the total phosphorus sources, with the main
367 coverage of the middle Yangtze Plain (i.e., Jiangxi and Anhui Province in Fig. 1), while class II cover
368 the most of lakes (n = 17) in the western regions (i.e., the Hunan Province and the western parts of the
369 Hubei Province in Fig. 1). The lakes of class III (n = 11) are primarily located on the eastern Yangtze
370 Plain, except for two lakes (i.e., Donghu and Tangxun lakes) which [located](#) at the urban area of Wuhan
371 City.

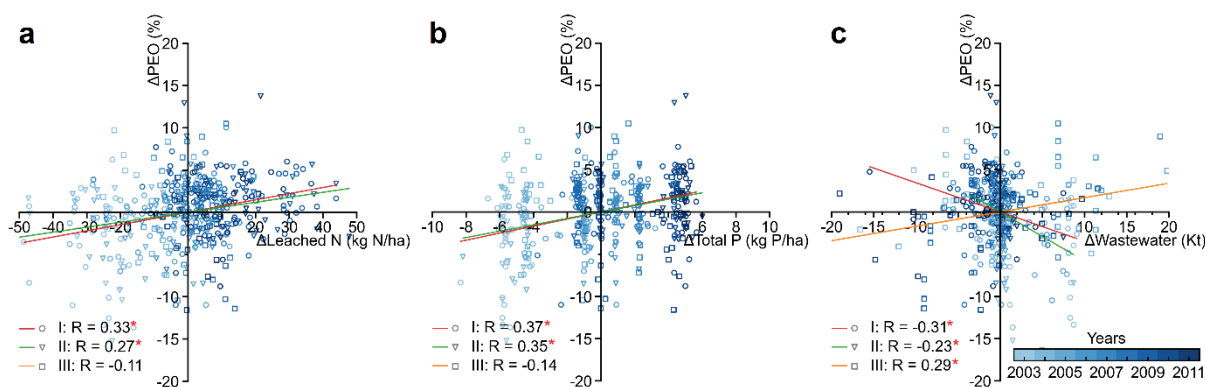
372 The correlations between annual anomalies of PEO and the three nutrient variables (relative to their
373 means for 2003-2011) were examined for all three lake classes. The PEO anomalies were significantly
374 correlated with different nutrient variables for three lake classes, indicating spatial variations of driving
375 factors for eutrophication changes on the Yangtze Plain (Fig. 8). Specifically, both LN and TP

376 anomalies exhibited significantly positive correlations ($p < 0.001$) with the PEO trends in lakes of class
 377 I and II (Fig. 8a&b), indicating that the primary influence of agriculture-related sources to the increasing
 378 trends of PEO. In contrast, the annual PEO dynamics in lakes of class III showed a significantly positive
 379 correlation ($p < 0.05$) with industrial wastewater discharge (Fig. 7e8c), meaning that the temporal trends
 380 of annual PEO in eastern parts of the Yangtze Plain were mainly associated with industrial wastewater
 381 discharge. Note that the significantly negative correlations between the PEO and IW anomalies were
 382 found for class I and II (Fig. 8c), which might be mechanistically unlikely. However, lakes in class I
 383 and II are mainly located in western and central regions, with intensive agriculture activities and high
 384 fertilizer applications (Chen et al., 2016). Such agriculture ecosystems provided substantial nutrient
 385 sources for eutrophication growth and development, greatly larger than available nutrient from
 386 industrial wastewater. In addition, agriculture nutrient sources generally increased with enhanced
 387 fertilizer applications, while industrial wastewater discharge showed overall decreasing trends (Li et al.,
 388 2013; Lyu et al., 2016). In such cases, industrial wastewater showed negative correlation with PEO
 389 anomalies for class I and II lakes. It was also acknowledged that such correlation between industrial
 390 wastewater and eutrophication changes might be affected by spatial variability in examined lakes within
 391 each class. more efforts are required in the future to determine the influence of industrial nutrient sources
 392 on eutrophication changes in these lakes.



393
 394 **Figure 7.** Loading plot of the principal component analysis (PCA) based on three nutrient-related
 395 variables. The color of scattering points represents the distributions of lakes in longitudinal order, and

396 the directions of nutrient-related variables (i.e., LN leached nitrogen; TP total phosphorus sources; IW
397 industrial wastewater) were annotated with blue arrows.



398
399 **Figure 8.** Relationships between the annual anomalies of PEO and nitrogen leaching (a), total
400 phosphorus sources (b), and industrial wastewater discharge (c) for fifty studied lakes. The color and
401 symbol of scattering points represent the years and lake classes, and the colored lines (shown for
402 significant correlations only) are linear regressions between the annual anomalies of PEO and
403 nutrient-related variables for each lake classes. Significant correlation coefficients are marked by
404 the red stars “*”.

405 4 Discussions

406 4.1 Significant decline in nitrogen use efficiency

407 The overall low mean NUE (27 %) and declining trends in NUE (-0.55 % yr⁻¹) characterized agricultural
408 ecosystems on the Yangtze Plain for the past four decades, which are consistent with previous studies
409 using statistical datasets and numerical modelling (Zhang et al., 2015; Yu et al., 2019). Over-
410 fertilization was primarily responsible for decline in NUE from 1979 to 2018 (Shi et al., 2020; Zhang
411 et al., 2015). Nitrogen fertilizer applications significantly increased by 2.5 times for past four decades,
412 greatly exceeding the increase magnitudes in crop production (+26.3%), which potentially contributed
413 to markedly decreasing NUE over the Yangtze Plain. Moreover, fertilization-induced increases of crop
414 yield always decrease with the increase in fertilizer applications, and eventually disappear when crop
415 yield reaches the upper limits (Zhang et al., 2015), suggesting that high fertilization rates are more likely
416 to generate the further decline in NUE over the Yangtze Plain. Over-fertilization might potentially
417 enhance nitrogen accumulation in soil that can be available for crop growth and development in next

418 years (Yang et al., 2006), thereby indicating that temporally increasing fertilization rates are generally
419 accompanied by declining NUE in agriculture ecosystems.

420 Considerable difference in NUE was examined among different crops, with the largest NUE values in
421 soybean for the past four decades (Fig. 5) as previously-documented NUE variations from 1961 to 2011
422 (Zhang et al., 2015). Generally, soybean has high NUEs mostly due to high protein contents (i.e., >
423 50%) in its grains (Fabre and Planchon, 2000). With the enhanced leaf nitrogen concentrations related
424 to its biological fixation, soybean tends to achieve a higher photosynthesis rate and delay leaf
425 senescence (Kaschuk et al., 2010; Ma et al., 2022), both of which potentially contributed to its generally
426 high NUE. Furthermore, double-cropping rice showed an overall lower NUE than single-season rice
427 (Fig. 5). It has been previously reported to occur in other double-cropping systems based on field
428 experiments, such as rice-wheat cropping (Liu et al., 2016b; Yi et al., 2015), rice-rapeseed cropping
429 (Wang et al., 2021a), and wheat-maize cropping (Xiao et al., 2021). Indeed, fertilizer applications
430 applied for the former crop could have accumulated nitrogen in soil that can be also taken by the latter
431 cultivated crop for their growth and development (Shi et al., 2020). In this regard, chemical fertilizer
432 applications for the latter crop can potentially generate the decline in its NUE.

433 **4.2 Primary causes of eutrophication changes.**

434 Our study revealed that the primary nutrient causes of eutrophication changes varied with regions over
435 the Yangtze Plain, where agricultural nutrient sources were strongly linked with eutrophication changes
436 in western and central lakes, while industrial wastewater showed a significantly positive correlation
437 with PEO trends in eastern lakes. Such spatial variations indicated that scientific policies and measures
438 were required to be implemented at local scales to mitigate eutrophication issues in lake ecosystems.
439 Separately, sustainable agriculture development should be encouraged to improve nitrogen/phosphorus
440 use efficiency and thus reduce agriculture nutrient sources available for western and central lakes to
441 potentially control eutrophication issues. In recent years, several agriculture practices have been
442 recommended and implemented, such as optimal fertilization schemes and residue removal, to pursue
443 high-efficiency agriculture on the Yangtze Plain (Cui et al., 2018; Shi et al., 2020). However,
444 smallholders were hesitant to adopt those knowledge-based practices, resulting in their poor
445 performance on agriculture sustainability (Cai et al., 2023). By contrast, national policies about

446 formulated fertilization was implemented in 2012, and fertilizer consumption started to decline since
447 2014 (Deng et al., 2021), which was expected to reduce agricultural nutrient sources in western and
448 central lakes.

449 ~~However, the generally low NUE constitutes a vast gap with the targeted sustainable NUE of 60% in~~
450 ~~China (Zhang et al., 2015), possibly leading to the excessive nitrogen discharge for terrestrial and~~
451 ~~aquatic ecosystems. The correlation analysis revealed that PEO trends in the western and central parts~~
452 ~~of the Yangtze Plain were associated with agricultural nutrient sources. As such, improving the NUE~~
453 ~~can decrease the agricultural nutrient exports to mitigate eutrophication issues in lake ecosystems,~~
454 ~~especially under the growing food demands in the future.~~

455 In the eastern parts of the Yangtze Plain, policies and measures about mitigating eutrophication issues
456 were suggested to mainly focus on the decline and treatment in industrial sewage due to its large
457 contributions to nutrient exports delivered to lakes from the adjacent cities. The Jiangsu Province in the
458 eastern parts of the Yangtze Plain (see the locations in Fig. 1) experienced rapid economic and industrial
459 development since the policy of Reform and Opening-up of China since 1980s (Shen et al., 2020),
460 suggesting that the associated industrial wastewater discharge might be enhanced and then discharge
461 substantial nutrients to phytoplankton communities in lake ecosystems. In such cases, various national
462 strategies and policies have been gradually implemented to promote the green growth of industries on
463 the Yangtze Plain. Considerable efforts were made to encourage the reclamation of wastewater,
464 investment in the advances in wastewater treatment technology and installment of municipal wastewater
465 treatment plants (Li et al., 2013; Lyu et al., 2016). Furthermore, industrial structures were also
466 encouraged to transform from secondary to tertiary industries under the environment-friendly targets of
467 economic development (Huang et al., 2015). All these measures were expected to contribute to the
468 decline in industrial sewage on the Yangtze Plain.

469 ~~the correlation between industrial wastewater and PEO indicates that industrial sewage possibly~~
470 ~~delivered terrestrial nutrients to lakes from the adjacent cities, providing sufficient nutrient conditions~~
471 ~~for phytoplankton communities (Luan et al., 2007). The Jiangsu Province in the eastern parts of the~~
472 ~~Yangtze Plain (see the locations in Fig. 1) experienced rapid economic and industrial development since~~

473 ~~the policy of Reform and Opening up of China since 1980s (Shen et al., 2020), which might be expected~~
474 ~~to result in enhanced industrial wastewater production, thereby triggering serious eutrophication in the~~
475 ~~lake systems. However, the national strategies and policies about green growth of industries encouraged~~
476 ~~reclamation of wastewater, investment on the advances in wastewater treatment technology and~~
477 ~~installment of municipal wastewater treatment plants (Li et al., 2013; Lyu et al., 2016). Industrial~~
478 ~~structures were also required to transform from secondary to tertiary industries under the environment-~~
479 ~~friendly targets of economic development (Huang et al., 2015). Consequently, industrial sewage showed~~
480 ~~decreasing trends and attributed to improvement of eutrophication status in the eastern Yangtze lakes.~~

4.3 Limitations and Uncertainties

Using the LPJ-GUESS model, we investigated the long-term changes and spatial variations of nitrogen dynamics (i.e., plant nitrogen uptake and nitrogen leaching) over the Yangtze Plain for the past four decades, and then examined the contributions of terrestrial nutrient sources to eutrophication changes in fifty large lakes. However, due to the lacking representation of a phosphorus cycle in the LPJ-GUESS model, we used external phosphorus fertilizer and manure application rates to represent the agricultural phosphorus sources, without consideration of potential impacts from plant and soil processes. Phosphorus fertilizer applications significantly increased from 6.5 kg P ha⁻¹ in 1980 to 22.0 kg P ha⁻¹ in 2014, and previous studies also reported that the overall low phosphorus use efficiency (< 40%) characterized the Yangtze Plain from 2001 to 2015 (Zheng et al., 2018), both of which were similar to nitrogen patterns on the Yangtze Plain for the past four decades. In addition, the leached nitrogen showed strong dependence on fertilizer applications ($R^2 = 0.92$, $p < 0.001$ in Fig. S4) over the Yangtze Plain for the past four decades. In this regard, we considered agricultural phosphorus sources as the potential driving force for eutrophication changes under the low levels of phosphorus use efficiency over the Yangtze Plain (Li et al., 2017; Zheng et al., 2018). Nevertheless, we also acknowledge that the use of phosphorus application data can generate uncertainties in our analysis, and thus processes related to phosphorus cycles are needed to add into LPJ-GUESS in the future to study the interactions of leached nitrogen and phosphorus on lake ecosystems.

~~Applied phosphorus is taken up through crop roots, or can be retained in soils (Schoumans, 2015) in variable degrees, affecting the export to lake ecosystems, which makes that the use of application data generates an uncertainty in our analysis. Nevertheless, we consider it important to consider the phosphorus sources as potential driving force for eutrophication changes under the low levels of phosphorus use efficiency over the Yangtze Plain (Li et al., 2017; Zheng et al., 2018).~~

Another source of uncertainty is associated with ~~the potential impacts of terrestrial nutrient losses during the transport processes that mediate the quantity and quality of terrestrial nutrients discharged the transport processes~~ to surface water ecosystems, as well as the impacts of aquaculture-related

507 nutrient sources. Lateral transport rates of runoff and dissolved matter~~Transport processes~~ depend on
508 soil properties, topography, and hydrological conditions over the drainage area (Solomon et al., 2015;
509 Tang et al., 2014; Tang et al., 2018), which is required to further consider at regional scales to estimate
510 link to the dynamics of terrestrial nutrient exports for lake ecosystems on the Yangtze Plain. In addition,
511 intensive and widespread freshwater aquaculture across the Yangtze Plain can contribute to accessible
512 nutrient sources for eutrophication development and phytoplankton growth (Guo and Li, 2003; Wang
513 et al., 2019a). Satellite observations revealed that 17 out of 50 lakes on the Yangtze Plain have
514 established enclosure fishery nets to increase fish production (Dai et al., 2019). Consequently,
515 substantial nutrients in fish food can directly enter aquaculture zones, promoting the contents of
516 nitrogen and phosphorus in these lakes. These associated drivers are required to be comprehensively
517 assessed to draw a complete picture of accessible nutrient sources for phytoplankton communities and
518 then specify the anthropogenic impacts on water quality and eutrophication deterioration on the Yangtze
519 Plain.

520 Uncertainties in the PEO data can originate from the uneven distributions of valid numbers of satellite
521 observations across the fifty large lakes of the Yangtze Plain. Under the influence of observational
522 conditions (i.e., cloud coverage and thick aerosols), the imagery with high-quality observations
523 distributed unevenly across the different years and seasons, which potentially resulted in certain impacts
524 on the derived annual PEOs and their temporal trends. Alternatively, the annual PEOs were calculated
525 based on the quarterly values to minimize such uncertainties. Nevertheless, more frequent satellite
526 observations (e.g., MODIS observations) will still be required to obtain a more accurate assessment of
527 eutrophication changes in lake ecosystems.

528 **5 Conclusions**

529 We used the LPJ-GUESS model to investigate the long-term changes of nitrogen dynamics over the
530 Yangtze Plain for the past four decades, and then examined their potential functions as the driving forces
531 of eutrophication changes in fifty large lakes of the Yangtze Plain. Significant decreases in NUE
532 dominated the whole Yangtze Plain, with the largest decrease in rice, soybean and rapeseed. The

533 leached nitrogen from both cropland and natural land showed statistically significant increasing trends
534 for all fifty examined lakes, indicating increased availability of terrestrial nitrogen sources in lake
535 systems for the past four decades. Two classes of lakes located in the western and central parts of the
536 Yangtze Plain showed significantly positive correlations between anomalies of PEO and agricultural
537 nutrient sources (i.e., the leached nitrogen and total phosphorus sources), and the PEO anomalies in the
538 remaining class (11 eastern lakes [in the eastern parts of the Yangtze Plain](#)) were positively correlated
539 with the industrial wastewater discharge. The impacts of agricultural and industrial nutrient sources [on](#)
540 eutrophication changes further emphasize [the importance of region-specific policies and measures \(i.e.,](#)
541 [sustainable management of agricultural nitrogen and phosphorus in western and central regions, and the](#)
542 [decline in wastewater-related nutrient discharge in eastern regions\) to improve water environments. ~~the~~
543 ~~importance of sustainable management of terrestrial nitrogen and phosphorus to improve water~~
544 ~~environments.~~](#)

545 *Data availability.* Data used in this study are archived by the authors and are available upon request.

546 *Author contributions.* QG, JT, LF and GS designed the framework and methodology of the study. QG
547 drafted [the](#) first version of the manuscript and analyzed the results. QG, JT and GS performed the
548 calibration of [the](#) LPJ-GUESS model. All co-authors contributed critically to the manuscript editing
549 and writing processes.

550 *Competing interests.* The authors declare that they have no conflict of interest.

551 [Acknowledgements.](#) This work was supported by the National Natural Science Foundation of China
552 (NOs: 41971304). Qi Guan was funded by the SUSTech-UCPH Joint Program. Jing Tang was
553 financially supported by Swedish FORMAS mobility grant (2016-01580) and MERGE Short project.
554 Stefan Olin acknowledges support from Lund University strong research areas MERGE and eSENCE.
555 We are grateful to the European Space Agency (ESA) for publishing land cover dataset and to the China
556 Meteorological Data Service Center for providing crop distribution and yield data.

557 **References**

558 Batjes, N. H.: Harmonized soil property values for broad-scale modelling (WISE30sec) with estimates
559 of global soil carbon stocks, *Geoderma*, 269, 61-68, 2016.

560 Cai, S., Zhao, X., Pittelkow, C. M., Fan, M., Zhang, X., and Yan, X.: Optimal nitrogen rate strategy for
561 sustainable rice production in China, *Nature*, 10.1038/s41586-022-05678-x, 2023.

562 Chen, F., Hou, L., Liu, M., Zheng, Y., Yin, G., Lin, X., Li, X., Zong, H., Deng, F., and Gao, J.: Net
563 anthropogenic nitrogen inputs (NANI) into the Yangtze River basin and the relationship with riverine
564 nitrogen export, *Journal of Geophysical Research: Biogeosciences*, 121, 451-465, 2016.

565 Chen, Q., Huang, M., and Tang, X.: Eutrophication assessment of seasonal urban lakes in China Yangtze
566 River Basin using Landsat 8-derived Forel-Ule index: A six-year (2013–2018) observation, *Science of
567 the Total Environment*, 745, 135392, 2020a.

568 Chen, S., Ge, Q., Chu, G., Xu, C., Yan, J., Zhang, X., and Wang, D.: Seasonal differences in the rice grain
569 yield and nitrogen use efficiency response to seedling establishment methods in the Middle and Lower
570 reaches of the Yangtze River in China, *Field Crops Research*, 205, 157-169, 2017.

571 Chen, X., Wang, L., Niu, Z., Zhang, M., and Li, J.: The effects of projected climate change and extreme
572 climate on maize and rice in the Yangtze River Basin, China, *Agricultural and Forest Meteorology*, 282,
573 107867, 2020b.

574 Chen, X., Strokal, M., Kroeze, C., Supit, I., Wang, M., Ma, L., Chen, X., and Shi, X.: Modeling the
575 contribution of crops to nitrogen pollution in the Yangtze River, *Environmental science & technology*,
576 54, 11929-11939, 2020c.

577 Cui, Z., Zhang, H., Chen, X., Zhang, C., Ma, W., Huang, C., Zhang, W., Mi, G., Miao, Y., and Li, X.: Pursuing
578 sustainable productivity with millions of smallholder farmers, *Nature*, 555, 363-366, 2018.

579 Dai, Y., Feng, L., Hou, X., Choi, C.-Y., Liu, J., Cai, X., Shi, L., Zhang, Y., and Gibson, L.: Policy-driven
580 changes in enclosure fisheries of large lakes in the Yangtze Plain: Evidence from satellite imagery,
581 *Science of the total environment*, 688, 1286-1297, 2019.

582 Defourny, P., Kirches, G., Brockmann, C., Boettcher, M., Peters, M., Bontemps, S., Lamarche, C., Schlerf,
583 M., and Santoro, M.: Land cover CCI, Product User Guide Version, 2, 325, 2012.

584 Deng, C., Liu, L., Peng, D., Li, H., Zhao, Z., Lyu, C., and Zhang, Z.: Net anthropogenic nitrogen and
585 phosphorus inputs in the Yangtze River economic belt: spatiotemporal dynamics, attribution analysis,
586 and diversity management, *Journal of Hydrology*, 597, 126221, 2021.

587 Fabre, F. and Planchon, C.: Nitrogen nutrition, yield and protein content in soybean, *Plant Science*, 152,
588 51-58, 2000.

589 Feng, L., Hou, X., and Zheng, Y.: Monitoring and understanding the water transparency changes of fifty
590 large lakes on the Yangtze Plain based on long-term MODIS observations, *Remote Sensing of
591 Environment*, 221, 675-686, 2019.

592 Gao, S., Xu, P., Zhou, F., Yang, H., Zheng, C., Cao, W., Tao, S., Piao, S., Zhao, Y., and Ji, X.: Quantifying
593 nitrogen leaching response to fertilizer additions in China's cropland, *Environmental pollution*, 211,
594 241-251, 2016.

595 Guan, Q., Feng, L., Hou, X., Schurgers, G., Zheng, Y., and Tang, J.: Eutrophication changes in fifty large
596 lakes on the Yangtze Plain of China derived from MERIS and OLCI observations, *Remote Sensing of
597 Environment*, 246, 111890, 2020.

598 Guo, L. and Li, Z.: Effects of nitrogen and phosphorus from fish cage-culture on the communities of a
599 shallow lake in middle Yangtze River basin of China, *Aquaculture*, 226, 201-212, 2003.

600 Hartigan, J. A. and Wong, M. A.: Algorithm AS 136: A k-means clustering algorithm, *Journal of the royal
601 statistical society. series c*, 28, 100-108, 1979.

602 He, J., Yang, K., Tang, W., Lu, H., Qin, J., Chen, Y., and Li, X.: The first high-resolution meteorological
603 forcing dataset for land process studies over China, *Scientific Data*, 7, 1-11, 2020.

604 Hou, X., Feng, L., Duan, H., Chen, X., Sun, D., and Shi, K.: Fifteen-year monitoring of the turbidity
605 dynamics in large lakes and reservoirs in the middle and lower basin of the Yangtze River, China,
606 *Remote Sensing of Environment*, 190, 107-121, 2017.

607 Hou, X., Feng, L., Tang, J., Song, X.-P., Liu, J., Zhang, Y., Wang, J., Xu, Y., Dai, Y., and Zheng, Y.:
608 Anthropogenic transformation of Yangtze Plain freshwater lakes: Patterns, drivers and impacts,
609 *Remote Sensing of Environment*, 248, 111998, 2020.

610 Hu, M., Ma, R., Xiong, J., Wang, M., Cao, Z., and Xue, K.: Eutrophication state in the Eastern China
611 based on Landsat 35-year observations, *Remote Sensing of Environment*, 277, 113057, 2022.

612 Huang, C., Zhang, M., Zou, J., Zhu, A.-x., Chen, X., Mi, Y., Wang, Y., Yang, H., and Li, Y.: Changes in land
613 use, climate and the environment during a period of rapid economic development in Jiangsu Province,
614 China, *Science of the Total Environment*, 536, 173-181, 2015.

615 Huang, J., Zhang, Y., Arhonditsis, G. B., Gao, J., Chen, Q., and Peng, J.: The magnitude and drivers of
616 harmful algal blooms in China's lakes and reservoirs: A national-scale characterization, *Water Research*,
617 181, 115902, 2020.

618 Huang, J., Zhang, Y., Arhonditsis, G. B., Gao, J., Chen, Q., Wu, N., Dong, F., and Shi, W.: How successful
619 are the restoration efforts of China's lakes and reservoirs?, *Environment international*, 123, 96-103,
620 2019.

621 Huang, M., Shan, S., Zhou, X., Chen, J., Cao, F., Jiang, L., and Zou, Y.: Leaf photosynthetic performance
622 related to higher radiation use efficiency and grain yield in hybrid rice, *Field Crops Research*, 193, 87-
623 93, 2016.

624 Kaschuk, G., Hungria, M., Leffelaar, P., Giller, K., and Kuyper, T.: Differences in photosynthetic
625 behaviour and leaf senescence of soybean (*Glycine max* [L.] Merrill) dependent on N₂ fixation or
626 nitrate supply, *Plant Biology*, 12, 60-69, 2010.

627 Lamarque, J. F., Dentener, F., McConnell, J., Ro, C. U., Shaw, M., Vet, R., Bergmann, D., Cameron-Smith,
628 P., Dalsoren, S., and Doherty, R.: Multi-model mean nitrogen and sulfur deposition from the
629 Atmospheric Chemistry and Climate Model Intercomparison Project (ACCMIP): evaluation of historical
630 and projected future changes, *Atmospheric Chemistry and Physics*, 13, 7997-8018, 2013.

631 Li, A. A., Stokal, M. M., Bai, Z. Z., Kroeze, C. C., Ma, L. L., and Zhang, F. F.: Modelling reduced coastal
632 eutrophication with increased crop yields in Chinese agriculture, *Soil Research*, 55, 506-517, 2017.

633 Li, H.-M., Tang, H.-J., Shi, X.-Y., Zhang, C.-S., and Wang, X.-L.: Increased nutrient loads from the
634 Changjiang (Yangtze) River have led to increased harmful algal blooms, *Harmful Algae*, 39, 92-101,
635 2014.

636 Li, S., Liu, C., Sun, P., and Ni, T.: Response of cyanobacterial bloom risk to nitrogen and phosphorus
637 concentrations in large shallow lakes determined through geographical detector: A case study of Taihu
638 Lake, China, *Science of The Total Environment*, 816, 151617, 2022.

639 Li, X. and Xiao, J.: A global, 0.05-degree product of solar-induced chlorophyll fluorescence derived from
640 OCO-2, MODIS, and reanalysis data, *Remote Sensing*, 11, 517, 2019.

641 Li, Y., Luo, X., Huang, X., Wang, D., and Zhang, W.: Life cycle assessment of a municipal wastewater
642 treatment plant: a case study in Suzhou, China, *Journal of cleaner production*, 57, 221-227, 2013.

643 Lindeskog, M., Arneeth, A., Bondeau, A., Waha, K., Seaquist, J., Olin, S., and Smith, B.: Implications of
644 accounting for land use in simulations of ecosystem carbon cycling in Africa, *Earth System Dynamics*,
645 4, 385-407, 2013.

646 Liu, X., Wang, H., Zhou, J., Hu, F., Zhu, D., Chen, Z., and Liu, Y.: Effect of N fertilization pattern on rice
647 yield, N use efficiency and fertilizer-N fate in the Yangtze River Basin, China, *PloS one*, 11, e0166002,
648 2016a.

649 Liu, X., Xu, S., Zhang, J., Ding, Y., Li, G., Wang, S., Liu, Z., Tang, S., Ding, C., and Chen, L.: Effect of
650 continuous reduction of nitrogen application to a rice-wheat rotation system in the middle-lower
651 Yangtze River region (2013–2015), *Field Crops Research*, 196, 348-356, 2016b.

652 Lu, C. and Tian, H.: Global nitrogen and phosphorus fertilizer use for agriculture production in the past
653 half century: shifted hot spots and nutrient imbalance, *Earth System Science Data*, 9, 181-192, 2017.

654 Luan, Q., Sun, J., Song, S., Shen, Z., and Yu, Z.: Canonical correspondence analysis of summer
655 phytoplankton community and its environment in the Yangtze River estuary, China, *Chinese Journal*
656 *of Plant Ecology*, 31, 445, 2007.

657 Lyu, S., Chen, W., Zhang, W., Fan, Y., and Jiao, W.: Wastewater reclamation and reuse in China:
658 opportunities and challenges, *Journal of Environmental Sciences*, 39, 86-96, 2016.

659 Ma, J., Olin, S., Anthoni, P., Rabin, S. S., Bayer, A. D., Nyawira, S. S., and Arneth, A.: Modeling symbiotic
660 biological nitrogen fixation in grain legumes globally with LPJ-GUESS (v4. 0, r10285), *Geoscientific*
661 *Model Development*, 15, 815-839, 2022.

662 Messager, M. L., Lehner, B., Grill, G., Nedeva, I., and Schmitt, O.: Estimating the volume and age of
663 water stored in global lakes using a geo-statistical approach, *Nature communications*, 7, 13603, 2016.

664 Olin, S., Schurgers, G., Lindeskog, M., Wårlind, D., Smith, B., Bodin, P., Holmér, J., and Arneth, A.:
665 Modelling the response of yields and tissue C: N to changes in atmospheric CO₂ and N management
666 in the main wheat regions of western Europe, *Biogeosciences*, 12, 2489-2515, 2015a.

667 Olin, S., Lindeskog, M., Pugh, T., Schurgers, G., Wårlind, D., Mishurov, M., Zaehle, S., Stocker, B. D.,
668 Smith, B., and Arneth, A.: Soil carbon management in large-scale Earth system modelling: implications
669 for crop yields and nitrogen leaching, *Earth System Dynamics*, 6, 745-768, 2015b.

670 Parton, W., Scurlock, J., Ojima, D., Gilmanov, T., Scholes, R., Schimel, D. S., Kirchner, T., Menaut, J. C.,
671 Seastedt, T., and Garcia Moya, E.: Observations and modeling of biomass and soil organic matter
672 dynamics for the grassland biome worldwide, *Global biogeochemical cycles*, 7, 785-809, 1993.

673 Parton, W. J., Hanson, P. J., Swanston, C., Torn, M., Trumbore, S. E., Riley, W., and Kelly, R.: ForCent
674 model development and testing using the Enriched Background Isotope Study experiment, *Journal of*
675 *Geophysical Research: Biogeosciences*, 115, 2010.

676 Piao, S., Ciais, P., Huang, Y., Shen, Z., Peng, S., Li, J., Zhou, L., Liu, H., Ma, Y., and Ding, Y.: The impacts
677 of climate change on water resources and agriculture in China, *Nature*, 467, 43-51, 2010.

678 Qin, B., Paerl, H. W., Brookes, J. D., Liu, J., Jeppesen, E., Zhu, G., Zhang, Y., Xu, H., Shi, K., and Deng, J.:
679 Why Lake Taihu continues to be plagued with cyanobacterial blooms through 10 years (2007–2017)
680 efforts, *Science Bulletin*, 64, 2019.

681 Qu, J. and Fan, M.: The current state of water quality and technology development for water pollution
682 control in China, *Critical reviews in environmental science & technology*, 40, 519-560, 2010.

683 Schoumans, O. F.: Phosphorus leaching from soils: process description, risk assessment and mitigation,
684 Wageningen University and Research 2015.

685 Shen, F., Yang, L., He, X., Zhou, C., and Adams, J. M.: Understanding the spatial–temporal variation of
686 human footprint in Jiangsu Province, China, its anthropogenic and natural drivers and potential
687 implications, *Scientific reports*, 10, 1-12, 2020.

688 Shi, X., Hu, K., Batchelor, W. D., Liang, H., Wu, Y., Wang, Q., Fu, J., Cui, X., and Zhou, F.: Exploring
689 optimal nitrogen management strategies to mitigate nitrogen losses from paddy soil in the middle
690 reaches of the Yangtze River, *Agricultural Water Management*, 228, 105877, 2020.

691 Sitch, S., Smith, B., Prentice, I. C., Arneth, A., Bondeau, A., Cramer, W., Kaplan, J. O., Levis, S., Lucht,
692 W., and Sykes, M. T.: Evaluation of ecosystem dynamics, plant geography and terrestrial carbon cycling
693 in the LPJ dynamic global vegetation model, *Global change biology*, 9, 161-185, 2003.

694 Smith, B., Wårlind, D., Arneth, A., Hickler, T., Leadley, P., Siltberg, J., and Zaehle, S.: Implications of
695 incorporating N cycling and N limitations on primary production in an individual-based dynamic
696 vegetation model, *Biogeosciences*, 11, 2027-2054, 2014.

697 Solomon, C. T., Jones, S. E., Weidel, B. C., Buffam, I., Fork, M. L., Karlsson, J., Larsen, S., Lennon, J. T.,
698 Read, J. S., and Sadro, S.: Ecosystem consequences of changing inputs of terrestrial dissolved organic
699 matter to lakes: current knowledge and future challenges, *Ecosystems*, 18, 376-389, 2015.

700 Tang, J., Pilesjö, P., Miller, P. A., Persson, A., Yang, Z., Hanna, E., and Callaghan, T. V.: Incorporating
701 topographic indices into dynamic ecosystem modelling using LPJ-GUESS, *Ecohydrology*, 7, 1147-1162,
702 2014.

703 Tang, J., Yurova, A. Y., Schurgers, G., Miller, P. A., Olin, S., Smith, B., Siewert, M. B., Olefeldt, D., Pilesjö,
704 P., and Poska, A.: Drivers of dissolved organic carbon export in a subarctic catchment: Importance of
705 microbial decomposition, sorption-desorption, peatland and lateral flow, *Science of the Total*
706 *Environment*, 622, 260-274, 2018.

707 Tilman, D., Balzer, C., Hill, J., and Befort, B. L.: Global food demand and the sustainable intensification
708 of agriculture, *Proceedings of the national academy of sciences*, 108, 20260-20264, 2011.

709 Tong, Y., Xiwen, X., Miao, Q., Jingjing, S., Yiyang, Z., Wei, Z., Mengzhu, W., Xuejun, W., and Yang, Z.:
710 Lake warming intensifies the seasonal pattern of internal nutrient cycling in the eutrophic lake and
711 potential impacts on algal blooms, *Water Research*, 188, 116570, 2021.

712 Tong, Y., Zhang, W., Wang, X., Couture, R.-M., Larssen, T., Zhao, Y., Li, J., Liang, H., Liu, X., and Bu, X.:
713 Decline in Chinese lake phosphorus concentration accompanied by shift in sources since 2006, *Nature*
714 *Geoscience*, 10, 507-511, 2017.

715 Wang, C., Yan, Z., Wang, Z., Batool, M., El-Badri, A. M., Bai, F., Li, Z., Wang, B., Zhou, G., and Kuai, J.:
716 Subsoil tillage promotes root and shoot growth of rapeseed in paddy fields and dryland in Yangtze
717 River Basin soils, *European Journal of Agronomy*, 130, 126351, 2021a.

718 Wang, D., Zhang, S., Zhang, H., and Lin, S.: Omics study of harmful algal blooms in China: Current status,
719 challenges, and future perspectives, *Harmful algae*, 107, 102079, 2021b.

720 Wang, J., Beusen, A. H., Liu, X., and Bouwman, A. F.: Aquaculture production is a large, spatially
721 concentrated source of nutrients in Chinese freshwater and coastal seas, *Environmental science &*
722 *technology*, 54, 1464-1474, 2019a.

723 Wang, L. and Davis, J.: Can China Feed its People into the Next Millennium? Projections for China's
724 grain supply and demand to 2100, *International Review of Applied Economics*, 12, 53-67, 1998.

725 Wang, M., Janssen, A. B., Bazin, J., Stokal, M., Ma, L., and Kroeze, C.: Accounting for interactions
726 between Sustainable Development Goals is essential for water pollution control in China, *Nature*
727 *communications*, 13, 1-13, 2022.

728 Wang, M., Stokal, M., Burek, P., Kroeze, C., Ma, L., and Janssen, A. B.: Excess nutrient loads to Lake
729 Taihu: Opportunities for nutrient reduction, *Science of the Total Environment*, 664, 865-873, 2019b.

730 Xiao, Q., Dong, Z., Han, Y., Hu, L., Hu, D., and Zhu, B.: Impact of soil thickness on productivity and
731 nitrate leaching from sloping cropland in the upper Yangtze River Basin, *Agriculture, Ecosystems &*
732 *Environment*, 311, 107266, 2021.

733 Xu, H., Paerl, H., Qin, B., Zhu, G., Hall, N., and Wu, Y.: Determining critical nutrient thresholds needed
734 to control harmful cyanobacterial blooms in eutrophic Lake Taihu, China, *Environmental science &*
735 *technology*, 49, 1051-1059, 2015.

736 Xu, X., Hu, H., Tan, Y., Yang, G., Zhu, P., and Jiang, B.: Quantifying the impacts of climate variability and
737 human interventions on crop production and food security in the Yangtze River Basin, China, 1990–
738 2015, *Science of the Total Environment*, 665, 379-389, 2019.

739 Yang, S.-M., Malhi, S. S., Song, J.-R., Xiong, Y.-C., Yue, W.-Y., Lu, L. L., Wang, J.-G., and Guo, T.-W.: Crop
740 yield, nitrogen uptake and nitrate-nitrogen accumulation in soil as affected by 23 annual applications
741 of fertilizer and manure in the rainfed region of Northwestern China, *Nutrient Cycling in*
742 *Agroecosystems*, 76, 81-94, 2006.

743 Yi, Q., He, P., Zhang, X., Yang, L., and Xiong, G.: Optimizing fertilizer nitrogen for winter wheat
744 production in Yangtze River region in China, *Journal of Plant Nutrition*, 38, 1639-1655, 2015.

745 Yu, C., Huang, X., Chen, H., Godfray, H. C. J., Wright, J. S., Hall, J. W., Gong, P., Ni, S., Qiao, S., and
746 Huang, G.: Managing nitrogen to restore water quality in China, *Nature*, 567, 516-520, 2019.

747 Yu, Q., Wang, F., Li, X., Yan, W., Li, Y., and Lv, S.: Tracking nitrate sources in the Chaohu Lake, China,
748 using the nitrogen and oxygen isotopic approach, *Environmental Science and Pollution Research*, 25,
749 19518-19529, 2018.

750 Zhang, B., Tian, H., Lu, C., Dangal, S. R., Yang, J., and Pan, S.: Global manure nitrogen production and
751 application in cropland during 1860–2014: a 5 arcmin gridded global dataset for Earth system
752 modeling, *Earth System Science Data*, 9, 667-678, 2017.

753 Zhang, C., Ju, X., Powlson, D., Oenema, O., and Smith, P.: Nitrogen surplus benchmarks for controlling
754 N pollution in the main cropping systems of China, *Environmental science & technology*, 53, 6678-
755 6687, 2019.

756 Zhang, M., Shi, X., Yang, Z., Yu, Y., Shi, L., and Qin, B.: Long-term dynamics and drivers of phytoplankton
757 biomass in eutrophic Lake Taihu, *Science of the Total Environment*, 645, 876-886, 2018.

758 Zhang, N., Gao, Z., Wang, X., and Chen, Y.: Modeling the impact of urbanization on the local and
759 regional climate in Yangtze River Delta, China, *Theoretical and applied climatology*, 102, 331-342, 2010.

760 Zhang, X., Davidson, E. A., Mauzerall, D. L., Searchinger, T. D., Dumas, P., and Shen, Y.: Managing
761 nitrogen for sustainable development, *Nature*, 528, 51-59, 2015.

762 Zhang, Y., Sun, M., Yang, R., Li, X., Zhang, L., and Li, M.: Decoupling water environment pressures from
763 economic growth in the Yangtze River Economic Belt, China, *Ecological Indicators*, 122, 107314, 2021.

764 Zhao, J., Luo, Q., Deng, H., and Yan, Y.: Opportunities and challenges of sustainable agricultural
765 development in China, *Philosophical Transactions of the Royal Society B: Biological Sciences*, 363, 893-
766 904, 2008.

767 Zhao, S., Chen, Y., Gu, X., Zheng, M., Fan, Z., Luo, D., Luo, K., and Liu, B.: Spatiotemporal variation
768 characteristics of livestock manure nutrient in the soil environment of the Yangtze River Delta from
769 1980 to 2018, *Scientific Reports*, 12, 1-17, 2022.

770 Zheng, J., Wang, W., Cao, X., Feng, X., Xing, W., Ding, Y., Dong, Q., and Shao, Q.: Responses of
771 phosphorus use efficiency to human interference and climate change in the middle and lower reaches
772 of the Yangtze River: historical simulation and future projections, *Journal of Cleaner Production*, 201,
773 403-415, 2018.

774 Zhu, Z., Bi, J., Pan, Y., Ganguly, S., Anav, A., Xu, L., Samanta, A., Piao, S., Nemani, R. R., and Myneni, R.
775 B.: Global data sets of vegetation leaf area index (LAI) 3g and fraction of photosynthetically active
776 radiation (FPAR) 3g derived from global inventory modeling and mapping studies (GIMMS) normalized
777 difference vegetation index (NDVI3g) for the period 1981 to 2011, *Remote sensing*, 5, 927-948, 2013.

778